



Università degli Studi Mediterranea di Reggio Calabria
Archivio Istituzionale dei prodotti della ricerca

Organic Matter Characterization and Phytotoxic Potential Assessment of a Solid Anaerobic Digestate Following Chemical Stabilization by an Iron-Based Fenton Reaction

This is the peer reviewed version of the following article:

Original

Organic Matter Characterization and Phytotoxic Potential Assessment of a Solid Anaerobic Digestate Following Chemical Stabilization by an Iron-Based Fenton Reaction / Roccotelli, Angela; Araniti, Fabrizio; Tursi, Antonio; Di Rauso Simeone, Giuseppe; Rao, Maria A; Lania, Ilaria; Chidichimo, Giuseppe; Abenavoli, Maria R; Gelsomino, Antonio. - In: JOURNAL OF AGRICULTURAL AND FOOD CHEMISTRY. - ISSN 0021-8561. - 68:35(2020), pp. 9461-9474. [10.1021/acs.jafc.0c03570]

Availability:

This version is available at: <https://hdl.handle.net/20.500.12318/64767> since: 2024-09-26T13:59:30Z

Published

DOI: <http://doi.org/10.1021/acs.jafc.0c03570>

The final published version is available online at: <https://pubs.acs.org/doi/abs/10.1021/acs.jafc.0c03570>

Terms of use:

The terms and conditions for the reuse of this version of the manuscript are specified in the publishing policy. For all terms of use and more information see the publisher's website

Publisher copyright

This item was downloaded from IRIS Università Mediterranea di Reggio Calabria (<https://iris.unirc.it/>) When citing, please refer to the published version.

(Article begins on next page)

05 February 2025

1 This is the peer reviewed version of the following article:

2

3 Angela Roccotelli, Fabrizio Araniti, Antonio Tursi, Giuseppe Di Rauso Simeone, Maria A. Rao, Ilaria

4 Lania, Giuseppe Chidichimo, Maria R. Abenavoli, Antonio Gelsomino

5

6 Organic matter characterization and phytotoxic potential assessment of a solid anaerobic digestate

7 following chemical stabilization by an iron-based Fenton reaction

8 J. Agric. Food Chem. 2020, 68, 9461–9474.

9 <https://dx.doi.org/10.1021/acs.jafc.0c03570>

10

11 The terms and conditions for the reuse of this version of the manuscript are specified in the publishing

12 policy. For all terms of use and more information see the publisher's website.

13

14

15

16

17

ACCEPTED MANUSCRIPT

18 **Organic matter characterization and phytotoxic potential assessment of a solid anaerobic**
19 **digestate following chemical stabilization by an iron-based Fenton reaction**

20

21 Angela Roccotelli[‡], Fabrizio Araniti[‡], Antonio Tursi[†], Giuseppe Di Rauso Simeone[§], Maria A. Rao[§],
22 Ilaria Lania[†], Giuseppe Chidichimo^{†§}, Maria R. Abenavoli[‡], Antonio Gelsomino^{‡*}

23

24

25 [‡]Department of Agricultural Sciences, Mediterranean University of Reggio Calabria, Feo di Vito,
26 89124 Reggio Calabria, Italy

27 [†]Department of Chemistry and Chemical Technologies, University of Calabria, Rende (CS), 87036,
28 Italy

29 [§]Department of Agricultural Sciences, University of Naples Federico II, Via Università 100, 80055
30 Portici, Italy

31 [§]Research Consortium TEBAID c/o Department of Chemistry and Chemical Technologies,
32 University of Calabria, Rende (CS), 87036, Italy

33

34

35

36

37 **Corresponding author**

38 * (A.G.) Department of Agricultural Sciences, Mediterranean University of Reggio Calabria, Feo di
39 Vito, 89124 Reggio Calabria, Italy. Phone: +39.0965.1694361. E-mail: agelsomino@unirc.it

40

41 **Abstract**

42 Digestates, the by-product of the anaerobic bioconversion of organic wastes for the production of
43 biogas, are highly variable in chemical and biological properties thus limiting their potential use in
44 agriculture as soil amendment. Using a lab-scale glass reactor we aimed to assess the feasibility to
45 chemically stabilize the solid fraction of an anaerobic digestate applying a Fenton reaction under
46 constant pH (3.0), temperature (70 °C), reaction time (8 h) and various combinations of H₂O₂ and
47 Fe²⁺. In Fenton-treated samples the phytotoxic potential (determined on a test plant), total phenols
48 and the bad smell odor index markedly declined, whereas total C and N remained unaltered.
49 Thermogravimetric (TG) analysis and Fourier transform infrared (FT-IR) spectroscopy revealed
50 contrasting changes in extracted humic and fulvic fractions being increased or depleted, respectively,
51 in aromatic substances. Process feasibility and optimum conditions for an effective biomass
52 stabilization were achieved with a H₂O₂/Fe²⁺ ratio between 0.02 and 0.03.

53
54 **Keywords:** biomass valorization; elemental analysis; FT-IR spectroscopy; humic-like compounds;
55 odor impact; post-digestion treatment; TG analysis; phenols.

56
57
58 **Introduction**

59 In recent years, sustainable processes of energy production have received an increased attention
60 among several governments across the European countries. In particular, a greater attention is being
61 devoted to the anaerobic digestion (AD) technology, which was originally developed for treating
62 biodegradable wastes and sewage sludge.^{1,2} The AD process relies upon the biological conversion of
63 organic by-products under low oxygen content for the production of a biogas, rich in methane (50-
64 80% v/v), together with carbon dioxide and other contaminant gases (i.e. H₂S). Biogas can be used
65 directly as a fuel, in combined heat and power gas engines, or upgraded to natural gas-quality
66 biomethane.³ Besides biogas, the AD process leads to the production of a partially degraded, nutrient-

67 rich by-product currently named digestate.⁴ Owing to its chemical composition and content of
68 essential plant nutrient elements – especially N-reduced forms and soluble potassium - anaerobic
69 digestate has the potential as soil conditioner to improve physical properties, and release soluble plant
70 nutrient elements thus reducing the supply of synthetic fertilizers.^{5,6} Moreover, it can increase soil C
71 storage⁷ and contribute to soil pest control.⁸ Nevertheless, a complete exhaustion of the AD process
72 is rarely achieved and, unless digestates undergo a proper post-processing treatment including
73 composting,⁹⁻¹¹ soil incorporation of yet unstable or immature by-product can negatively affect the
74 soil-plant system.¹⁰ Most known undesirable features are: high levels of heavy metals,¹² phytotoxic
75 compounds,¹³ pathogenic bacteria,¹⁴ bad odor emission, unbalanced nutrient content and excess
76 inorganic N forms. As well as this, recent European¹⁵ and National¹⁶ regulations together with local
77 guidelines have established the maximum annual amounts of anaerobic digestate to be incorporated
78 into arable fields to protect groundwater from nitrate contamination. Therefore, anaerobic digestates
79 need to be fully stabilized and characterized for their residual phytotoxicity and chemical composition
80 before their safe use in agricultural systems.

81 Although known for more than one century, the Fenton reaction (first described by H.J.H. Fenton¹⁷
82 and based on Fe²⁺-catalyzed H₂O₂ decomposition in strongly oxidizing hydroxyl radicals) was not
83 applied in environmental protection technologies until the late 1960s. Nowadays the classical Fenton
84 reaction is considered as one of a set of advanced oxidation processes (AOPs)^{18,19} and is widely used
85 for the chemical treatment of wastewater, industrial sludge, landfill leachate, soils and sediments
86 which are contaminated with biorefractory organic compounds such as phenols, dyes, pesticides,
87 organic solvents, pharmaceuticals, domestic chemicals, etc.²⁰⁻²⁴ Popularity and widespread
88 applications of the Fenton oxidation process are due to the following features: 1) it works at near-
89 ambient temperature and pressure conditions, 2) it requires cheap, relatively reactive and easy-to
90 handle reagents, 3) it is rapid and effective, and 4) it can be easily integrated in more sophisticated
91 chemical technologies for the treatment of a broad range of hazardous wastes, including solid
92 agricultural matrices such as digestates from AD plants. Although few studies have recently

93 approached the chemical stabilization of the anaerobic digestate,²⁵⁻²⁷ they primarily focused on
94 dewaterability and changes in the chemical characteristics of treated organic wastes. Whereas no
95 attempt has been made to assess the phytotoxic potential and investigate specific changes in
96 spectroscopic features of digestate-derived humic-like compounds, which are key to restoring the
97 fertility level once incorporated into arable soils. Aim of the present work was to assess the
98 effectiveness of an iron-based Fenton reaction as a fast and low-cost, post-digestion, chemical
99 technology to stabilize the solid fraction of an anaerobic digestate, reduce its phytotoxic potential and
100 promote the formation of humic-like compounds, thus providing suitable features for its safe use in
101 agriculture for managing the fertility of soil. To this aim, we employed a lab-scale glass reactor to
102 investigate various combinations of reduced H₂O₂ and Fe²⁺ dosages on physical (bad odor emission),
103 chemical (total phenols, organic matter, electrical conductivity) and phytotoxic properties of a solid
104 anaerobic digestate. Fenton-treated digestates and their extracted humic and fulvic fractions were also
105 characterized by elemental analysis, FT-IR spectroscopy and TG analysis. Findings from the research
106 represent the first step towards Fenton process optimization in real plants for AD by-products
107 stabilization.

108

109 **Materials and Methods**

110 **Anaerobic digestate**

111 The anaerobic digestate was provided by a local full-scale biogas producing plant (Fattoria della Piana
112 soc. Agricola, RC, Italy) fed with an ingestate constituted by a mix of dairy cattle slurry, as the major
113 component, together with milk serum, maize silage and, in minor amount, olive waste and citrus pulp.
114 The rated power of the plant was 999 kWh with a hydraulic retention time (HRT) of 60 days in two
115 continuously stirred tank reactors (CSTR) of a total capacity of 7500 m³ (2500 m³ tank reactor 1 +
116 5000 m³ tank reactor 2), operating under mesophilic conditions (40 °C). The total volume loaded per
117 day was 120 m³, the hydraulic retention time (HRT) 60 days, and the minimum guaranteed retention
118 time (MGRT) 16 h at 40 °C. The digestate used in the present research was subjected to mechanical

119 solid/liquid separation (by press screw) to separate the aqueous fraction (named liquor), which was
120 discarded, from the solid fraction which was collected and then characterized (Table 1) as previously
121 described^{4,12} before use. Briefly, the electrical conductivity (EC) and pH were measured in a
122 biomass/water (1:10) and (3:50) (w/v) mixture, respectively. The ash content was determined after
123 combustion at 550 °C for 8 h, whereas total organic C and total N were measured by an automatic
124 elemental analyzer CN628 LECO (LECO Corporation, USA). NH₄⁺-N and NO₃⁻-N contents in 2 M
125 KCl extracts (1:10 v/v) were determined colorimetrically by using a Flow Injection Analysis System
126 (FIAS 400 PerkinElmer, Inc., CT, USA) equipped with an AS90 Autosampler (PerkinElmer) and
127 linked to an UV/Vis spectrophotometer Lambda 25 (PerkinElmer). Total K, S, Ca, Mg, Cl, F, Mn, B,
128 Cd, Cr, Pb, Ni, Hg, Cu and Zn were determined by inductively coupled plasma mass spectrometry
129 (ICP-MS ICAP-Q Thermo Scientific, CA) after microwave (Ethos up, Milestones srl, I) acid
130 digestion with HNO₃/H₂O₂ (7:1 v/v). Enzymatic (alkaline phosphatase, dehydrogenase and
131 hydrolysis of fluorescein diacetate) activities were determined colorimetrically.²⁸ All analyses were
132 carried out in triplicate.

133

134 **Iron-based Fenton reaction**

135 The iron-based Fenton oxidation of the solid anaerobic digestate was carried out using a laboratory-
136 scale glass reactor apparatus (Figure S1). Freshly sampled solid anaerobic digestate (equivalent to
137 100 g dry weight) was finely ground (particle size < 3 mm) and then placed into the glass reactor
138 together with the Fenton reagents: Fe²⁺ (as the catalyst) provided in form of high purity epta-hydrate
139 ferrous sulfate (FeSO₄·7H₂O, 99.5% purity) (VEBI Istituto Biochimico s.r.l., Italy) and analytical
140 grade hydrogen peroxide solution (H₂O₂, 30% w/w) (Panreac Applichem, Spain) (as the oxidant),
141 which was properly diluted to the desired final concentration. Reagent dosage and H₂O₂/Fe²⁺ ratio of
142 the differing treatments as well as Fenton reaction operating conditions were as detailed in Table 2.
143 A stirring devise was properly adapted to fit the glass reactor and maintain the mixture under
144 continuous stirring at 50 rpm. The air-tight glass reactor was placed into a water bath set at 70 °C. An

145 internal pressure gradient of -100 mbar, respect to ambient pressure, was maintained throughout the
146 entire process so as to allow the sample to become completely dry. The pH mixture was allowed
147 declining to pH 3.0 and maintained until the reaction had completed. The reaction took as long as 8
148 hours to complete, when any repelling odor was no longer appreciable and the mixture reached a
149 complete dryness. To sum up, ten chemically and thermally treated (A1-A5, B1-B5) and one
150 thermally treated samples with no reagent addition (Ctrl) were produced during the Fenton
151 stabilization process, and then immediately stored in air-tight bags before any further analysis.
152 Untreated solid anaerobic digestate was oven-dried at 105 °C until constant weight and taken as a
153 reference treatment (Dig).

154

155 **Extraction of humic-like fractions**

156 Fulvic (FA) and humic (HA) acids were extracted and fractionated as described previously.²⁹ Briefly,
157 an amount of the organic matrix equivalent to 2 g dry weight was transferred into a 250-mL Teflon
158 centrifuge tube containing 100 mL of 0.1 M NaOH and 0.1 M Na₄P₂O₇ solution. The headspace of
159 each tube was flushed with N₂ to create an anaerobic environment, and then the tubes were shaken
160 (80 rpm) at 65 °C for 24 h. The suspension was centrifuged at 6000 rpm for 20 min and filtered
161 through a 0.80 µm membrane filter. An aliquot of 25 mL of the filtered extract was acidified to pH 2
162 with diluted H₂SO₄ (1:1 in water) to separate HA from FA. Following centrifugation (6000 rpm, 20
163 min), pelleted HA were collected, while the supernatant containing FA was further purified by
164 passing it through a 10 cm³ of an insoluble polyvinylpyrrolidone resin (Fluka Analytical) equilibrated
165 with 0.005 M H₂SO₄. The eluate containing the non-humified fraction was discarded, while the
166 retained fraction was eluted with 0.5 M NaOH and collected. HA and FA fractions were freeze-dried
167 and stored at -20 °C before any further characterization.

168

169 **Odor emission**

170 Odor emission from either dry (immediately after the oxidation treatment) or rewetted (few weeks
171 after the treatment) Fenton-treated and control samples was estimated by a panel test made up of five
172 people using the following class rating system of bad odor emission: class 1 (no perception), class 2
173 (light perception), 3 (very strong perception). The mean value of the scores given to each treatment
174 has been reported as BSI (Bad Smell Index).

175

176 **Chemical analyses**

177 The electrical conductivity (EC) of Fenton-treated and control samples was measured in a
178 biomass/water (1:10, w/v) mixture; whereas the total phenolic compounds (TPC) content was
179 determined as described before.³⁰ Briefly, a suitable amount (0.500 g) of the organic matrix was
180 extracted with ethyl acetate under shaking at room temperature for 16 h. The extract was concentrated
181 by evaporation under vacuum (LABOROTA 4000, Heidolph, D) and then dissolved in 5 mL of
182 methanol. Content of TPC in the extracts was determined by using the Folin-Ciocalteu reagent (Sigma,
183 Italy). Briefly, 20 μL of the digestate extract was added with distilled water (830 μL), the Folin-
184 Ciocalteu reagent (50 μL) and, after 3 minutes 100 μL of 6% (w/v) NaOH. Following 1 h incubation,
185 the content of TPC was determined spectrophotometrically at 725 nm. Analytical readings were
186 expressed as mg of catechol equivalent per kg dry weight. The determination of organic matter (OM)
187 content of Fenton digestates was done by loss on ignition according to the method 5A described in
188 the Kellogg Soil Survey Laboratory Methods Manual.³¹ Elemental C and N contents in Fenton
189 digestates and their extracted humic-like fractions were determined by an automatic elemental
190 analyzer CN628 LECO (LECO Corporation, USA). All the chemical analyses were carried out in
191 triplicate.

192

193 **FT-IR analysis**

194 Fourier-transform infrared (FT-IR) spectroscopy analysis of Fenton-treated and control samples and
195 their extracted HA and FA fractions was performed in the wavenumber range of 400-4000 cm^{-1} by

196 using a Spectrum One FT-IR spectrometer (PerkinElmer, CT, USA). One milligram of each organic
197 sample was ground up with 400 mg KBr (FT-IR grade) and homogenized in an agate mortar. KBr
198 pellets were compressed under vacuum, under a pressure of 10000 kg cm⁻² for 10 min. Thirty-two
199 scans were collected and corrected against a control pellet containing only KBr.

200

201 **TG analysis**

202 Thermogravimetric (TG) analysis of dried and milled Fenton-treated and control samples and their
203 extracted HA and FA fractions (5 mg dry weight) was performed by using a Simultaneous Thermal
204 Analyser (STA) 6000 PerkinElmer (PerkinElmer, CT, USA) operating within the range 30 - 900 °C
205 at a heating rate of 15 °C min⁻¹, under synthetic air atmosphere (21 ± 1% O₂ and 79 ± 1% N₂ at a 100
206 mL min⁻¹ flow rate). TG profiles and differential thermogravimetry (DTG) curves were obtained in
207 terms of the percentage of weight loss of the sample and from the first derivative of TG profiles
208 representing the rate of weight loss, respectively. In order to obtain the real organic matter content
209 (C_{corr}), the weight loss attributed to the residual water was subtracted from DTG peaks (DTG2 and
210 DTG3) as follows:

$$211 \quad C_{corr} = 100 \cdot \left(\frac{C_i}{100 - C_{water}} \right) \quad (1)$$

212 where C_i is the weight loss of peak DTG2 or DGT3 registered in the DTG profiles (as an example,
213 the DTG profile of Dig is reported in Figure S2), and C_{water} is the first DTG peak (DTG1) occurring
214 to 60 °C and corresponds to the dehydration of the residual water content.³²

215

216 **Phytotoxicity assay**

217 The phytotoxic assay of either the native or Fenton-treated solid anaerobic digestate was carried out
218 in accordance to previously described³³ adopting a completely randomized design with five
219 replications. Briefly, Fenton-treated digestates were extracted with water (1:20, w/v, on dry weight
220 basis) under shaking (120 rpm) at room temperature for 24 h. Then, the suspension was filtered

221 (Whatman[®] no. 42) and the extract was diluted with sterile distilled water so as to obtain the following
222 concentrations: 0, 0.1, 1, 5, 10, 20, 80, and 100%. Germination and root growth of lettuce (*Lactuca*
223 *sativa* L.) seeds exposed to the digestate aqueous extracts were evaluated. Briefly, lettuce seeds were
224 surface-sterilized by soaking in 15% (v/v) NaClO solution for 15 minutes and then rinsed with
225 distilled water. Ten seeds were evenly distributed into a Petri dish (Ø 6 cm), on a double layer of
226 filter paper previously moistened with 2 mL of each dilution of the aqueous extract. Petri dishes were
227 then placed in the dark into a growth chamber at 24 ± 1 °C and 70% relative humidity. After 48 hours,
228 germinated seeds were counted and their root length measured by using a WinRhizo pro STD 1600
229 software (Instruments Régent Inc, Canada). The Germination Index [GI (%)] was calculated by
230 multiplying the germination percentage by the root length percentage, divided by 100 as reported
231 before.³⁴

232

233 **Statistical analysis**

234 Chemical data shown in Tables 3 and 4 are reported as mean values ($n = 3$), and a Tukey's honest
235 significant difference (HSD) post hoc test was run to compare means at a $P < 0.05$ level of significance.
236 Data from the phytotoxic assay (Figures 4 and 5) were first tested for deviation from normality
237 (Kolmogorov-Smirnov test) and homogeneity of within-group variances (Levene's test). After
238 running a one-way ANOVA to check any significant effect of the treatment (extract dose) on the
239 variability of the data (the block effect in the experimental design was found to be not significant at
240 $P < 0.05$), multiple pairwise comparison of means was done by Tukey's HSD test at $P < 0.05$ level of
241 significance. In order to compare the effects of aqueous extracts from differently treated digestates, a
242 non-linear regression model based on a log-logistic function³⁵ was used to estimate ED₅₀ values,
243 which represents the percent extract dose lowering the maximum GI (%) by 50%. The model
244 parameters were estimated by the least square method (TableCurve 2D v.4.0 software, Jandel
245 Scientific Ekrath, D) using the Levenburg-Marquardt algorithm for fitting non-linear equations. Non-
246 linear regressions were repeated several times in order to minimize the sum of the square of deviation

247 between the predicted and experimental values to less than 0.01% between two consecutive fits. The
248 quality of curve fitting was assessed by *F* test for non-fit based on analysis of variance at $P < 0.05$.
249 Statistical analyses were performed using the Systat 13.0 version 13.1 software package (SYSTAT
250 Software Inc.).

251

252 **Results**

253 **Solid anaerobic digestate characterization**

254 Chemical characterization of the digestate (Table 1) showed a slightly high dry mass content ($> 30\%$),
255 but still consistent with what generally found in final products from AD of agroindustrial wastes.^{5,10}
256 The final biomass showed an alkaline reaction, as expected, because volatile fatty acids degradation
257 and ammonia production occurring during the AD process leads to an increase of the pH.⁴ Low values
258 of EC and ash content were also found, thus indicating that the soluble salts did not represent a
259 limiting factor for agricultural use of the by-product. The digestate showed also an interesting content
260 of macronutrients (namely K and S) and a low concentration of inorganic contaminants (particularly
261 Cd, Pb, Ni, Hg, Cu and Zn), which were in compliance with mandatory limits. However, the Cr(VI)
262 content was almost five-fold the limit value according to the Italian legislation,¹⁶ whereas it was only
263 slightly above the current limit of 2 mg kg^{-1} reported in the recently approved Regulation EU n.
264 1009/2019.¹⁵ Noticeably, most N occurred as organic form (ammonium-N was approximately $\sim 12\%$
265 of total N), whereas the nitrate-N content was negligible. Total C was in accordance to literature,^{36,37}
266 while a considerably high (17.86%) content of humified fractions ($C_{\text{HA}} + C_{\text{FA}}$) was found.
267 Nonetheless, this latter finding was consistent with the observed BOD_5 value lower than 2.5 g L^{-1}
268 (Table 1) thus designating an anaerobic digestate suitable for use as fertilizer also in accordance with
269 Albuquerque et al.⁵ Even though the C/N ratio was higher than 25 (Table 1), once incorporated into
270 the soil the mineralization of the more labile organic fractions could lead to the release of soluble-N
271 forms. Finally, the residual biomass showed noticeable enzymatic activities; whereas levels of

272 microorganisms harmful to human health (*Salmonella* spp., *Escherichia coli*) were below the
273 detectable threshold.

274

275 **Characterization of Fenton-treated digestate**

276 Data from the BSI panel test clearly show that a H₂O₂ dosage equal or greater than 18.9 mg L⁻¹
277 provided conditions suitable for stabilization as observed for treatments A4, A5, B4, and B5, that
278 reached a score as low as 1 (Table 3). This condition is achieved at both Fe²⁺ catalyst concentration
279 levels: 846 and 1692 mg L⁻¹. However, the higher the Fe²⁺ catalyst, the lower the stability in terms of
280 odor emission as in the case of Fenton-treated digestates B2 and B3 vs A2 and A3 (Table 3). This
281 finding suggests that beside a proper single catalyst dosage, also a H₂O₂/Fe²⁺ ratio larger than 0.01 is
282 equally decisive for ensuring optimum conditions for the Fenton oxidation process. Expectedly, no
283 reduction in the BSI was found when one or both catalysts were omitted (Table 3). It is interesting to
284 note that this finding is consistent with the larger amount of HA and FA recovered in samples A4,
285 A5, B4, and B5, which appeared also to be chemically stabilized.

286 The EC of the Fenton-treated samples significantly increased with increasing the catalytic Fe²⁺
287 dosage used during the oxidative process (i.e. control samples < treatments A < treatments B).
288 Moreover, within the same iron dosage an increasing trend was found along with the H₂O₂
289 concentration increased (Table 3).

290 The TPC content in Fenton-treated digestates was strongly influenced by the oxidative treatments. In
291 particular, it declined significantly by 31% in the thermally-treated control (Ctrl) compared to the
292 untreated solid anaerobic digestate (Dig, 363.2 mg catechol kg⁻¹) (Table 3). A further significant
293 decrease of TPC was observed after the Fenton reaction, and this decline was especially linked to the
294 increasing dosage of H₂O₂ (from 0 to 24.12 mg L⁻¹) rather than that of catalytic Fe²⁺ (from 846 to
295 1692 mg L⁻¹), which indeed did not bring about any TPC reduction (Table 3).

296 The amount of organic matter in the biomass was not influenced by the oxidation process, and it
297 ranged from 88.8% to 91.7% with no significant differences among treatments.

298 As for the elemental composition, the iron-based Fenton treatment did not affect the total C and N
299 content despite the reagents dosage or their $\text{H}_2\text{O}_2/\text{Fe}^{2+}$ ratio (Table 3), with the only exception
300 represented by the Ctrl treatment that showed the larger elemental N content. The C/N ratio varied
301 accordingly: the samples B1, B4, and B5 were characterized by a C/N value greater than that of Dig
302 and particularly of the other samples (Table 3).

303

304 **Humic and fulvic fractions of digestates**

305 The iron-based Fenton process influenced the extraction yield and altered considerably the elemental
306 C and N content of extracted HA and FA (Table 4). In brief, the thermal treatment at 70 °C induced
307 a slight, but negligible, increase of the HA extraction yield. The same did not occur for FA where
308 yield raised from 0.9% of control native digestate (Dig) to 2.7% of thermally treated sample Ctrl
309 (Table 4). Moreover, increasing amounts of H_2O_2 enhanced the HA yield, but this trend was more
310 evident at the lowest Fe^{2+} dosage (846 mg L^{-1}) and at a $\text{H}_2\text{O}_2/\text{Fe}^{2+}$ ratio larger than 0.01: HA yields in
311 samples B3, B4, and B5 were always lower than those found in samples A3, A4, and A5 (Table 4).
312 A similar trend was also evidenced in the FA extraction yield that reached the highest values in A4
313 and B4 treatments (Table 4).

314 Elemental C and N contents in extracted HA remained practically unchanged in Dig and Ctrl
315 treatments, while they decreased significantly in all Fenton-treated digestates. In particular, the
316 smaller the $\text{H}_2\text{O}_2/\text{Fe}^{2+}$ ratio of the catalysts used during the process, the lesser the C content found in
317 the HA fractions (Table 4). Moreover, treatments with similar $\text{H}_2\text{O}_2/\text{Fe}^{2+}$ ratios (i.e. A2 and B3, A3,
318 and B5) showed the smaller C content was observed when the larger Fe^{2+} catalyst dosage was applied
319 (Table 4). On the other hand, a declining trend of elemental N content of extracted HA was observed
320 in all Fenton-treated digestates, particularly in those from samples treated with the greater catalytic
321 Fe^{2+} dosage (Table 4).

322 Conversely, elemental C and N contents in extracted FA followed a slightly different trend, and they
323 declined considerably in all samples, including Ctrl, when compared to Dig (Table 4). Precisely, a

324 decreasing C content was observed in FA extracted from samples treated with a smaller $\text{H}_2\text{O}_2/\text{Fe}^{2+}$
325 ratio of catalysts used during the process. Noticeably, the N trend distanced itself from that of the C
326 content: N sensitively decreased in FA extracted from Fenton digestates treated at greater $\text{H}_2\text{O}_2/\text{Fe}^{2+}$
327 ratios (Tables 2 and 4).

328

329 **FT-IR spectroscopy**

330 The FT-IR spectra of Fenton-treated digestates and control samples are reported in Figure 1. Relevant
331 peaks assigned to special functional groups and compounds are summarized in Table 5. The FT-IR
332 analysis from native and Fenton-treated digestates evidenced peaks of OH of phenols, alcohols and
333 carboxylic groups ($3300\text{-}3400\text{ cm}^{-1}$) and C–H stretching of alkyl structures ($2847\text{-}2955\text{ cm}^{-1}$). The
334 absorbance bands at $1710\text{-}1772\text{ cm}^{-1}$ and $1590\text{-}1686\text{ cm}^{-1}$ were assigned to C=O stretching in
335 carboxyl groups, carboxylic acids and ketones and aromatic C=C, C=O in amides I, ketone and
336 quinone groups, respectively. In particular, the peak at 1738 cm^{-1} raised by increasing both Fe^{2+} and
337 H_2O_2 rate. The absorbance bands at $1508\text{-}1560\text{ cm}^{-1}$ and $1444\text{-}1460\text{ cm}^{-1}$ were assigned to N–H
338 stretching of amide II and C–H stretching in aliphatic structures, respectively. At $1370\text{-}1381\text{ cm}^{-1}$ the
339 peak related to COO^- antisymmetric stretching, C–H and bending of CH_2 and CH_3 groups of amide
340 III or aromatic ethers was observed (Figure 1). The absorbance band at $1100\text{-}1270\text{ cm}^{-1}$ was assigned
341 to C–O stretching of aryl ethers and phenols, and to C–O stretching of secondary alcohols. The peak
342 at 1040 cm^{-1} was attributed to C–O stretching of polysaccharides. In all spectra the absorption bands
343 at $874\text{-}896\text{ cm}^{-1}$ were assigned to C–O bonds in the carbonate ion.^{32,38–40}

344 The FT-IR spectra of HA and FA extracted from Fenton-treated digestates and control samples are
345 shown in Figure 2. Precisely, FT-IR analysis of HA evidenced two peaks at 2931 cm^{-1} and at 2954
346 cm^{-1} , which were attributed to C–H stretching of alkyl structures (Figure 2a). These peaks were more
347 pronounced in HA from Dig than in those from Fenton-treated digestates. The shoulder at 1720 cm^{-1}
348 assigned to C=O stretching in carboxyl groups, carboxylic acids and ketones was observed only in
349 HA from Dig control sample. Moreover, Dig spectra showed a greater relative intensity of peaks at

350 1510 and 1460 cm^{-1} assigned to amide II of N–H stretching and C–H stretching of aliphatic structures,
351 respectively (Figure 2a). The peak at 1600 cm^{-1} assigned to aromatic C=C, C=O in amides I, ketone,
352 and quinone groups was more intensive in HA extracted from Fenton treated samples (Figure 2a). In
353 the spectra the adsorption at 1198 cm^{-1} assigned to C–O stretching and OH deformation of COOH^{38,40}
354 appeared in the HA extracted from treatments B2 and B4. In addition, the peak at 1125 cm^{-1} ,
355 corresponding to C–O stretching of aryl ethers and phenols, C-O stretching of secondary alcohols,
356 was more intensive in treatment A1, B1, B2 and B3. In particular, in sample B3 the signal drew two
357 bands (1120 cm^{-1} and 1140 cm^{-1})^{32,38–40} (Figure 2a).

358 As regards FT-IR analysis of FA, only FT-IR spectra of samples A1 and B1, where 846 and 1492 mg
359 L^{-1} of Fe^{2+} was applied in the Fenton oxidation, respectively, showed the peak at 1381 cm^{-1} assigned
360 to COO^- antisymmetric stretching, C–H and bending of CH_2 and CH_3 groups (Figure 2b). The C–O
361 stretching and OH deformation of COOH at 1198 cm^{-1} was observed only in the samples Ctrl, B1,
362 B2, B4, and B5 (Figure 2b). Furthermore, peaks at 1120 cm^{-1} and 1090 cm^{-1} , assigned to C–O
363 stretching of aryl ethers and phenols, C–O stretching of secondary alcohols, increased in intensity in
364 Ctrl and in Fenton treated A1, A2, B1, B2, B4, and B5 samples. The same peaks disappeared in A3,
365 A4, A5, and B3 samples (Figure 2b).

366

367 **TG analysis**

368 Three different peaks were registered in DTG profiles in according to Wu et al.³² The peak DTG1 at
369 60 °C was mainly associated to the dehydration of samples, whereas the peak DTG2 registered within
370 the temperature range of 200-350 °C was attributed to the thermal degradation of readily degradable
371 materials and semi-volatile compounds, such as carbohydrates, aliphatic structures, carboxylic groups,
372 hemicellulose, cellulose, and microbial cell walls. The peak DTG3 observed within the range of 400-
373 600 °C was associated to the thermal decomposition of aromatic and polynuclear structures of high
374 molecular weight. The DTG2 and DTG3 peaks were corrected by subtracting the weight loss due to
375 the residual water.

376 The corrected weight loss of DTG2 and DTG3 of reference untreated and Fenton-treated digestates
377 is showed in Figure 3a. No difference between Dig and Ctrl samples was observed in DTG2 peak,
378 while a slight increase (from 6.9% to 7.6%) in DTG3 peak was measured. DTG2 peak decreased in
379 all treatments A and B except in A5 (the greatest $\text{H}_2\text{O}_2/\text{Fe}^{2+}$ ratio), which showed a bigger peak than
380 Dig (+18.3%) and Ctrl (+16.6%), and in B1 (no H_2O_2 addition) that remained unchanged respect to
381 Dig and Ctrl. Conversely, DTG3 peak decreased as the $\text{H}_2\text{O}_2/\text{Fe}^{2+}$ ratio was increased during the
382 Fenton reaction, especially at lower Fe^{2+} dosage, until to reach 3.5% in A5. Whereas at the greater
383 Fe^{2+} concentration (samples B) no peak DTG3 change was noticed except in B1 where the peak value
384 increased (9.1%).

385 TG analysis of HA extracted from Fenton-treated digestates indicated that HA of Ctrl produced
386 greater DTG2 and DTG3 peaks than HA from Dig (Figure 3b). No further increase of peak DTG2
387 was found in HA from Fenton-treated digestates, except in HA from treatments B4 and B5 (11.7 and
388 11.5%, respectively). DTG3 peak increased in HA extracted from A1 and remained nearly unchanged
389 in other samples A respect to Ctrl. Samples B were also characterized by DTG3 peaks similar to those
390 of Ctrl. Extracted FA produced thermograms having DTG2 peaks more pronounced than those of
391 both Dig and Ctrl; whereas DTG3 peaks appeared strongly depleted in all treatments, including Ctrl
392 that underwent only the thermal treatment without catalyst addition, and the A5 treatment (highest
393 $\text{H}_2\text{O}_2/\text{Fe}^{2+}$ ratio) which showed the lowest value (Figure 3c).

394

395 **Phytotoxicity assay**

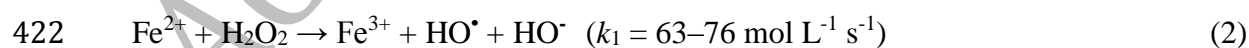
396 The untreated solid anaerobic digestate (Dig) exerted a considerable phytotoxic potential as shown
397 by the dose response curve (Figure 4). In particular, significant GI (%) inhibition (by about 11%) was
398 noticeable already at low digestate extract dose (namely 1%) and this inhibiting effect increased along
399 with the increasing extract concentration until reaching a 54% inhibition at the highest value (Figure
400 4). The ED_{50} value was 74.36%, thus confirming the phytotoxic potential of the aqueous extract from
401 Dig. Interestingly, the phytotoxic response to the aqueous extract changed significantly in relation to

402 the $\text{H}_2\text{O}_2/\text{Fe}^{2+}$ dosage used in the Fenton oxidation process. In details, the thermal treatment with no
403 chemical reagent addition (Ctrl) decreased, at least partially, the phytotoxic potential of the residual
404 biomass, which showed a slight stimulatory action at lower dosages and a phytotoxic response only
405 at the highest concentration (Figure 5). No phytotoxic potential of the aqueous digestate extracts arose
406 after the chemical treatment of solid digestate at the $846 \text{ mg L}^{-1} \text{ Fe}^{2+}$ dosage, despite the hydrogen
407 peroxide concentration applied within the experimental range (Figure 5). Conversely, a stimulatory
408 action was observed at 100% extract dosage: GI (%) values showed an increasing trend from 116.44
409 ± 7.5 (in treatment A2) to $152.65 \pm 8.0\%$ (in treatment A4) with an average value equal to $131.48 \pm$
410 22.5% . On the other side, the aqueous extracts from solid anaerobic digestate treated with an
411 increased Fe^{2+} dosage (1692 mg L^{-1}) showed a clear phytotoxic action on seed germination and root
412 growth of lettuce (Figure 5). Noticeably, there was an increased phytotoxic response to the treated
413 matrix as long as the hydrogen peroxide concentration increased in the Fenton oxidation process,
414 which became evident and extended over the entire dilution range when using a concentration of
415 H_2O_2 larger than 18.9 mg L^{-1} (Figure 5). In the presence of the 100% extract the GI value ranged
416 from 76.82% (treatment B2) to 94.37% (treatment B5).

417

418 Discussion

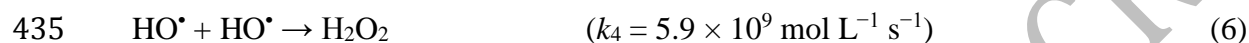
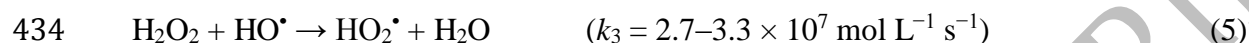
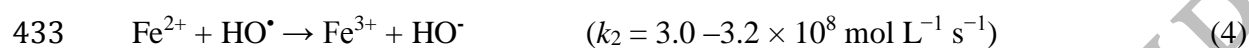
419 According to most researchers,^{18,41,42} Fenton chemistry encompasses the activation of hydrogen
420 peroxide (H_2O_2) by ferrous (Fe^{2+}) ions to generate hydroxyl radicals (HO^\bullet) under acidic conditions
421 *via* a complex reaction sequence, following the chain initiation reaction (Eq. 2):



423 In the presence of an organic substrate (R-H) the hydroxyl radical abstracts a hydrogen atom from R-
424 H and generates an organic radical (R^\bullet), which then undergoes a series of chemical transformations
425 to form various oxidation products (Eq. 3):



427 The hydroxyl radical is the main reactant of the Fenton oxidation process, capable of reacting with
428 organic substrates via oxidation. Even though the use of excess concentration of Fe^{2+} and H_2O_2 should
429 theoretically allow a complete conversion of all organic compounds into CO_2 and water, the
430 occurrence of various competitive processes due to non-specific reactivity of HO^\bullet towards both
431 organic and inorganic substrates negatively affects the organic oxidation process, thus leading to
432 chain termination (Eq. 4-6):



436 Although H_2O_2 is rapidly regenerated though Eq. (6), scavenging of HO^\bullet by Fe^{2+} catalyst (Eq. 4) may
437 reduce the overall oxidation efficiency. It is also true that the hydroperoxyl radical HO_2^\bullet produced in
438 reaction (Eq. 5) can reduce Fe^{3+} to Fe^{2+} , but because k_3 (Eq. 5) is an order of magnitude lower than
439 k_2 (Eq. 4), Fe^{2+} catalyst is being decreased during the reaction. Thus, profiling the concentration of
440 applied H_2O_2 and Fe^{2+} catalyst as well as their $\text{H}_2\text{O}_2/\text{Fe}^{2+}$ ratio is crucial to maximize the efficiency
441 of the process depending on the organic waste to treat.

442 H_2O_2 represents the dominant source of hydroxyl radicals, limitations in its concentration can
443 severely affect the process efficiency, and most contributes to increase the treatment costs. Whereas
444 Fe^{2+} catalyst requires dosages that strongly vary with the type and amount of waste to treat and has
445 major advantages like natural abundance, environmental compatibility, low-toxicity, high reactivity
446 and reduced commercial cost.^{21,43} As to assess the feasibility of the efficiency of the post-digestion
447 Fenton treatment of solid anaerobic digestate very small dosages of H_2O_2 (ranging from 6,03 to 24,12
448 mg L^{-1}) with relatively large amounts of catalytic Fe^{2+} (precisely 846 and 1692 mg L^{-1}) were here
449 investigated. Most promising results were obtained when considering a hydrogen peroxide
450 concentration not less than 18,09 mg L^{-1} with iron dosage not less than 846 mg L^{-1} , thus giving a
451 $\text{H}_2\text{O}_2/\text{Fe}^{2+}$ ratio larger than 0.02. Contrarily to what reported for chemically treating organic wastes
452 dispersed in aqueous systems,^{22,23} larger amounts of catalytic Fe^{2+} were here requested for the process

453 efficiency, since lower concentrations of catalytic Fe^{2+} produced no stabilization effect. We
454 hypothesize that in our system constituted by a partially hydrated solid matrix of individual highly
455 heterogeneous millimetric-sized organic particles the Fenton process was mainly controlled by the
456 diffusion rate and persistence of the catalysts into the biomass, thus requiring larger Fe^{2+} ion
457 concentrations.

458 The efficiency of a classical Fenton reaction depends also on pH, temperature, and reaction time.²¹
459 Even though contrasting conclusions have been reached, the optimum pH range for effective waste
460 treatment appears to be 2.5-3.0,¹⁹ as maintained in the present study. In fact, acid pH leads to the
461 dissolution of ferric ions and hydroxyl radical, allowing the H_2O_2 stabilization and resulting in
462 prolonged activity.⁴³ The treatment efficiency can be improved by increasing the temperature, which
463 can provide more energy to overcome the reaction activation energy. Generally, 25-40 °C represents
464 the most used temperature range for the Fenton process; however, higher temperatures (> 40 °C) can
465 be also applied depending on the nature of the waste material to treat.⁴⁴ Our previous investigations
466 on solid-state organic matrices (i.e. sewage sludge) have shown that 70 °C provided optimum
467 conditions for the oxidative treatment. A reaction time ranging from 20 to 60 min is required in most
468 cases even though prolonged reaction times (up to 240 min) were experienced for efficient treatments
469 of recalcitrant organic wastes (i.e. olive-oil mill waste).⁴³ In the present experiment a reaction time
470 as long as 8 hours is actually the combination of an expected shorter reaction time, due to the nearly
471 solid state consistency of the treated material, and the need to allow the material to reach a complete
472 dryness as well as absence of any repelling odor emission. In fact, shorter reaction times would
473 produce materials retaining the original repelling odor, or which become gradually bad smelling after
474 re-hydration of the final products. Confirming that application of a higher gradient of negative
475 pressure during the reaction can help the sample reach complete dryness, but not an optimal
476 stabilization.

477 Under our experimental conditions, TPC in Fenton-treated digestates decreased considerably, and
478 this decline, apparently linked to increasing the catalyst dosage, became particularly evident when

479 the $\text{H}_2\text{O}_2/\text{Fe}^{2+}$ ratio was > 0.01 . This finding confirms what previously reported⁴⁵ that the oxidation
480 of organic contaminants increases at increasing $\text{H}_2\text{O}_2/\text{Fe}^{2+}$ ratios. Interestingly, neither the total C nor
481 the total N varied during the process, suggesting that non-intense oxidation conditions occurred
482 during the process. Further inside, TG analysis showed that samples treated with increasing H_2O_2
483 dosage at $846 \text{ mg L}^{-1} \text{ Fe}^{2+}$ (samples A, greater $\text{H}_2\text{O}_2/\text{Fe}^{2+}$ ratio) the recalcitrant fraction (DTG3 peak)
484 declined as also previously observed.⁴⁶ On the other hand, at the greatest Fe^{2+} dosage (samples B,
485 lower $\text{H}_2\text{O}_2/\text{Fe}^{2+}$ ratio), the recalcitrant fraction was not affected. This finding suggests that rather
486 than inducing more oxidative conditions, a major catalytic iron concentration could have led to a
487 “scavenging effect” of the HO^\bullet radical (Eq. 4) with a consequent reduced efficiency of the oxidative
488 process, as also postulated by Wu et al.⁴⁶ Interestingly, samples treated only with Fe^{2+} catalyst
489 evidenced an increase of the recalcitrant fraction (DTG3 peak; Figure 3), especially at the greatest
490 dosage where ferrous ions could have become complexed with humic substances. In fact, at acidic
491 pH, Fe^{2+} is adsorbed onto carboxylic groups of humic fractions.^{47,48} Unlike extracted humic fractions—
492 as reported below, no differences arose in FT-IR spectra of Fenton-treated digestates with no
493 alteration of aliphatic groups, aromatic, ketone and quinone groups, and polysaccharides after the
494 oxidation process, in contrast with Quina et al.²⁵, though they adopted more intense oxidative
495 conditions (i.e. $\text{H}_2\text{O}_2 > 5 \text{ g kg}^{-1}$ total solid).

496 Conversely, thermal treatment, catalysts dosage and the $\text{H}_2\text{O}_2/\text{Fe}^{2+}$ ratio clearly affected yields and
497 properties of both HA and FA extracted from Fenton-stabilized digestates. In fact, following the
498 thermal treatment (Ctrl) an increased amount of both HA and FA was extracted, that continued to
499 grow up by increasing the $\text{H}_2\text{O}_2/\text{Fe}^{2+}$ ratio during the reaction. This behavior could be explained by
500 the combined thermal treatment and complexation of Fe^{2+} onto HA and FA, that leads to a stable
501 humic fraction.^{47,48} However, as long as the oxidative condition increased – due to the increasing
502 $\text{H}_2\text{O}_2/\text{Fe}^{2+}$ ratio – lesser N was being incorporated into the humic-like fractions particularly FA. We
503 surmise that the greater abundance of ferric ions generated by the large amount of H_2O_2 could have
504 acted as a Lewis acid, thus promoting the catalytic cleavage of peptide bonds, release of amino acids

505 and major loss of N, which was not incorporated into the final FA product. In a few words, yields and
506 properties of humic-like fractions were the result of a combination of oxidative and hydrolytic
507 reactions determined by both highly reactive hydroxyl radicals and catalytic ferric ions.

508 The major impact of the Fenton process became clear analysing the FT-IR spectra of extracted HA.
509 In fact, the signals attributed to alkyl structures, amides and polysaccharides appeared reduced, and
510 also those of carboxylic groups resulted depleted after treatment. Conversely, FT-IR spectra showed
511 an increase of aromatic structures and groups as aryl ethers, phenols, and secondary alcohols thereby
512 indicating HA from Fenton-stabilized digestates as more stable products. This behavior was also
513 confirmed by the TG analysis. In fact, the recalcitrant fraction, associated to the thermal
514 decomposition of aromatic structures within the range of 400-600 °C, enlarged respect to HA from
515 non-treated digestate (Dig). In according to the theory of the supramolecular structure of humic
516 substances proposed by Piccolo,⁴⁹ the presence of Fe²⁺ promoted thermodynamically stable
517 associations due to the complexation with acidic functional groups of humic molecules, thus losing
518 their previous weakly-held conformations.⁴⁹

519 Conversely, FA extracted appeared depleted in aromatic structures but enriched in aryl ethers and
520 phenols, and secondary alcohols, as shown in FT-IR spectra and confirmed by TG analysis. In other
521 words, the more recalcitrant fractions (DTG3 peaks) strongly decreased respect to Dig, whereas the
522 more labile fraction (DTG2 peaks) increased. During the Fenton stabilization process, when both
523 oxidative and hydrolytic reactions occurred, recalcitrant compounds could be transformed in more
524 labile ones: Nuzzo et al.⁴⁸ found that Fe addition leads to the formation of highly hydrated and poorly
525 associated fulvic molecules.

526 Contrasting results have been reported as regards digestates phytotoxicity, ranging from absence⁵⁰ to
527 strong⁵¹ phytotoxic responses on germination and growth of *Lepidium sativum*. In accordance with
528 latter results, our Dig inhibited the lettuce germination at concentrations $\geq 1\%$ reaching a $\sim 50\%$ of
529 inhibition at the largest concentration. As suggested by several authors, the GI inhibition could be
530 attributed to a high content of organic matter^{52,53} and soluble salts as they can negatively affect the

531 water uptake needed for germination.⁵⁴ However, since the EC significantly increased in all the
532 treated digestates, including those which were not phytotoxic, the influence of an unfavorable osmotic
533 potential on seed germination and seedling growth was here considered negligible. On the other hand,
534 phenolic compounds, alone or in complex mixture, can exert phytotoxic effects on both germination
535 and seedling establishment, even at low concentrations.⁵⁵ As seen before, TPC strongly varied with
536 reagent dosage and their combination, suggesting that the differences in phytotoxic responses can be
537 strictly correlated with the TPC of the organic matrix. Interestingly, a stimulatory effect on the GI
538 parameter was also observed, especially at the lowest concentrations. This phenomenon, known as
539 hormesis, is generally induced by the phenolic acids, which show a dualistic behaviour, being
540 stimulatory at low and inhibitory at high concentrations.^{56,57} Both the TPC and phytotoxic potential
541 of Fenton-treated digestates declined at the lowest Fe^{2+} catalyst dosage and when the $\text{H}_2\text{O}_2/\text{Fe}^{2+}$ ratio
542 increased, while a larger HA content was observed. We hypothesize that increased humic-like
543 substances could have contributed to stimulate the germination and seedlings growth of lettuce, also
544 as reported before.⁵⁸

545 To sum up, this lab scale study showed that Fenton post-digestion treatment has great potential for
546 large-scale application in increasing stability and detoxication of solid anaerobic digestates, whose
547 agricultural valorization as soil amendment is severely constrained by residual phytotoxic potential
548 and instability. We found it out that a reduced H_2O_2 dosage between 18.9 and 24.12 mg L^{-1} and an
549 amount of Fe^{2+} catalyst slightly large but not exceeding 846 mg L^{-1} , at pH 3.0 and 70 °C for 8 h under
550 continuous stirring at 50 rpm, represent the optimum conditions to produce an effective biomass
551 stabilization. The resulting $\text{H}_2\text{O}_2/\text{Fe}^{2+}$ ratio ranging from 0.02 and 0.03, which is certainly small when
552 compared to those used in wastewater treatment, is in agreement with that suggested by Nieto et al.⁵⁹

553 Given the properties of the matrix to treat, this reagent ratio has been found suitable for decreasing
554 the phytotoxic potential and total phenols, and increasing the stability of the product as well as the
555 content and the structure of chemically-induced formation of humic-like fractions, which can be
556 beneficial to soil properties. Nevertheless, it is also worth noting that the C/N ratio of the stabilized

557 product remains somewhat high (> 25) thus requiring additional inorganic N supply for avoiding
558 microbial N immobilization when the stabilized material is being used as soil amendment.

559

560 **Funding**

561 The research received the financial support of the POR Calabria FESR 2007/2013 within the frame
562 of the project Si.Re.Ja. (CUP J14E07000400005) addressed to state and private enterprises joining
563 the Regional Technological Innovation Centre for the “Renewable Energy, Energetic Efficiency and
564 Technologies for the Sustainable Management of Environmental Resources” - Polo NET.

565

566 **Abbreviations used**

567 AD, anaerobic digestion; AOP, advanced oxidation process; BSI, bad smell index; CSTR,
568 continuously stirred tank reactor; DTG, differential thermogravimetry; EC, electrical conductivity;
569 FT-IR, Fourier-transform infrared spectroscopy; FA, fulvic acids; GI, germination index; HA, humic
570 acids; HRT, hydraulic retention time; MGRT, minimum guaranteed retention time; OM, organic
571 matter; TG, thermogravimetric; TPC, total phenolic compounds

572

573 **References**

- 574 (1) Appels, L.; Baeyens, J.; Degrève, J.; Dewil, R. Principles and potential of the anaerobic
575 digestion of waste-activated sludge. *Prog. Energy Combust. Sci.* **2008**, *34* (6), 755–781.
- 576 (2) Tursi, A. A review on biomass: importance, chemistry, classification, and conversion.
577 *Biofuel Res. J.* **2019**, *6* (2), 962–979.
- 578 (3) Chynoweth, D. P.; Owens, J. M.; Legrand, R. Renewable methane from anaerobic digestion
579 of biomass. *Renew. Energy* **2001**, *22* (1–3), 1–8.
- 580 (4) Tambone, F.; Genevini, P.; D’Imporzano, G.; Adani, F. Assessing amendment properties of
581 digestate by studying the organic matter composition and the degree of biological stability
582 during the anaerobic digestion of the organic fraction of MSW. *Bioresour. Technol.* **2009**,

- 583 100 (12), 3140–3142.
- 584 (5) Alburquerque, J. A.; de la Fuente, C.; Ferrer-Costa, A.; Carrasco, L.; Cegarra, J.; Abad, M.;
585 Bernal, M. P. Assessment of the fertiliser potential of digestates from farm and agroindustrial
586 residues. *Biomass Bioenerg.* **2012**, *40*, 181–189.
- 587 (6) Insam, H.; Gómez-Brandón, M.; Ascher, J. Manure-based biogas fermentation residues -
588 Friend or foe of soil fertility? *Soil Biol. Biochem.* **2015**, *84*, 1–14.
- 589 (7) Grigatti, M.; Di Girolamo, G.; Chincarini, R.; Ciavatta, C.; Barbanti, L. Potential nitrogen
590 mineralization, plant utilization efficiency and soil CO₂ emissions following the addition of
591 anaerobic digested slurries. *Biomass Bioenerg.* **2011**, *35* (11), 4619–4629.
- 592 (8) Fernández-Bayo, J. D.; Achmon, Y.; Harrold, D. R.; McCurry, D. G.; Hernandez, K.;
593 Dahlquist-Willard, R. M.; Stapleton, J. J.; VanderGheynst, J. S.; Simmons, C. W.
594 Assessment of two solid anaerobic digestate soil amendments for effects on soil quality and
595 biosolarization efficacy. *J. Agric. Food Chem.* **2017**, *65* (17), 3434–3442.
- 596 (9) Abdullahi, Y. A.; Akunna, J. C.; White, N. A.; Hallett, P. D.; Wheatley, R. Investigating the
597 effects of anaerobic and aerobic post-treatment on quality and stability of organic fraction of
598 municipal solid waste as soil amendment. *Bioresour. Technol.* **2008**, *99* (18), 8631–8636.
- 599 (10) Teglia, C.; Tremier, A.; Martel, J.-L. Characterization of solid digestates: part 2, assessment
600 of the quality and suitability for composting of six digested products. *Waste Biomass*
601 *Valorization* **2011**, *2* (2), 113–126.
- 602 (11) Fuchs, W.; Drosch, B. Assessment of the state of the art of technologies for the processing of
603 digestate residue from anaerobic digesters. *Water Sci. Technol.* **2013**, *67* (9), 1984–1993.
- 604 (12) Bonetta, S.; Bonetta, S.; Ferretti, E.; Fezia, G.; Gilli, G.; Carraro, E. Agricultural reuse of the
605 digestate from anaerobic co-digestion of organic waste: microbiological contamination,
606 metal hazards and fertilizing performance. *Water, Air Soil Pollut.* **2014**, *225* (8), 1–11.
- 607 (13) Levén, L.; Nyberg, K.; Schnürer, A. Conversion of phenols during anaerobic digestion of
608 organic solid waste – A review of important microorganisms and impact of temperature. *J.*

- 609 *Environ. Manage.* **2012**, 95, S99–S103.
- 610 (14) Sahlström, L. A review of survival of pathogenic bacteria in organic waste used in biogas
611 plants. *Bioresour. Technol.* **2003**, 87 (2), 161–166.
- 612 (15) Regulation (EU) 1009/2019 of the European Parliament and of the Council of 5 June 2019
613 laying down rules on the making available on the market of EU fertilising products and
614 amending regulations (EC) No. 1069/2009 and (EC) No. 1107/2009 and repealing regulation
615 (EC) No. 2003/2003. *Off. J. Eur. Comm.* **2019**, L170/1, 1–114.
- 616 (16) D. Lgs. 29 aprile 2010, n. 75. “Riordino e revisione della disciplina in materia di fertilizzanti,
617 a norma dell’articolo 13 della legge 7 luglio 2009, n. 88,” *Gazzetta Ufficiale della*
618 *Repubblica Italiana*, **2010**, 121, Suppl. Ord. n. 106/L.
- 619 (17) Fenton, H. J. H. Oxidation of tartaric acid in presence of iron. *J. Chem. Soc. Trans.* **1894**, 65,
620 899–910.
- 621 (18) Pignatello, J. J.; Oliveros, E.; MacKay, A. Advanced oxidation processes for organic
622 contaminant destruction based on the Fenton reaction and related chemistry. *Crit. Rev.*
623 *Environ. Sci. Technol.* **2006**, 36 (1), 1–84.
- 624 (19) Neyens, E.; Baeyens, J. A review of classic Fenton’s peroxidation as an advanced oxidation
625 technique. *J. Hazard. Mater.* **2003**, 98 (1–3), 33–50.
- 626 (20) Babuponnusami, A.; Muthukumar, K. A review on Fenton and improvements to the Fenton
627 process for wastewater treatment. *J. Environ. Chem. Eng.* **2014**, 2 (1), 557–572.
- 628 (21) Wang, N.; Zheng, T.; Zhang, G.; Wang, P. A review on Fenton-like processes for organic
629 wastewater treatment. *J. Environ. Chem. Eng.* **2016**, 4 (1), 762–787.
- 630 (22) Mirzaei, A.; Chen, Z.; Haghghat, F.; Yerushalmi, L. Removal of pharmaceuticals from
631 water by homo/heterogonous Fenton-type processes – A review. *Chemosphere* **2017**, 174,
632 665–688.
- 633 (23) Lu, M. C.; Lin, C. J.; Liao, C. H.; Huang, R. Y.; Ting, W. P. Dewatering of activated sludge
634 by Fenton’s reagent. *Adv. Environ. Res.* **2003**, 7 (3), 667–670.

- 635 (24) Dulova, N.; Trapido, M. Application of Fenton's reaction for food-processing wastewater
636 treatment. *J. Adv. Oxid. Technol.* **2011**, *14* (1), 9–16.
- 637 (25) Quina, M. J.; Lopes, D. V.; Cruz, L. G.; Andrade, J.; Martins, R. C.; Gando-Ferreira, L. M.;
638 Dias-Ferreira, C.; Quinta-Ferreira, R. M. Studies on the chemical stabilisation of digestate
639 from mechanically recovered organic fraction of municipal solid waste. *Waste Biomass*
640 *Valorization* **2015**, *6* (5), 711–721.
- 641 (26) Innocenzi, V.; Zammartino, A.; Mazziotti di Celso, G.; Chianese, S.; Musmarra, D.;
642 Prisciandaro, M. Simulation of a real plant for the combined treatment of wastewaters and
643 liquid wastes. *Desalin. Water Treat.* **2018**, *108*, 198–206.
- 644 (27) Wang, Q.; Sun, J.; Song, K.; Zhou, X.; Wei, W.; Wang, D.; Xie, G. J.; Gong, Y.; Zhou, B.
645 Combined zero valent iron and hydrogen peroxide conditioning significantly enhances the
646 dewaterability of anaerobic digestate. *J. Environ. Sci. (China)* **2018**, *67*, 378–386.
- 647 (28) Dick, R. P.; Breakwell, D. P.; Turco, R. F. Soil enzyme activities and biodiversity
648 measurements as integrative microbiological indicators. In *Methods for Assessing Soil*
649 *Quality*; Doran, J. W., Jones, A. J., Eds.; SSSA: Madison, WI, USA, 1997; SSSA Special
650 Publications No. 49, pp 247–271.
- 651 (29) Ciavatta, C.; Govi, M.; Vittori Antisari, L.; Sequi, P. Characterization of humified
652 compounds by extraction and fractionation on solid polyvinylpyrrolidone. *J. Chromatogr. A*
653 **1990**, *509* (1), 141–146.
- 654 (30) Greco, G. Jr.; Colarieti, M. L.; Toscano, G.; Iamarino, G.; Rao, M. A.; Gianfreda, L.
655 Mitigation of olive mill wastewater toxicity. *J. Agric. Food Chem.* **2006**, *54* (18), 6776–
656 6782.
- 657 (31) Soil Survey Staff. *Kellogg soil survey laboratory methods manual. Soil survey investigations*
658 *report No. 42, Version 5.0.*; R. Burt and Soil Survey Staff, Ed.; U.S. Department of
659 Agriculture, Natural Resources Conservation Service. **2014**; pp 495-497.
- 660 (32) Wu, H.; Zhao, Y.; Long, Y.; Zhu, Y.; Wang, H.; Lu, W. Evaluation of the biological stability

- 661 of waste during landfill stabilization by thermogravimetric analysis and Fourier transform
662 infrared spectroscopy. *Bioresour. Technol.* **2011**, *102* (20), 9403–9408.
- 663 (33) Gelsomino, A.; Abenavoli, M. R.; Princi, G.; Attinà, E.; Cacco, G.; Sorgonà, A. Compost
664 from fresh orange waste: A suitable substrate for nursery and field crops? *Compost Sci. Util.*
665 **2010**, *18* (3), 201–210.
- 666 (34) Murillo, J. M.; Cabrera, F.; López, R.; Martín-Olmedo, P. Testing low-quality urban
667 composts for agriculture: germination and seedling performance of plants. *Agric. Ecosyst.*
668 *Environ.* **1995**, *54* (1–2), 127–135.
- 669 (35) Araniti, F.; Lupini, A.; Mercati, F.; Statti, G. A.; Abenavoli, M. R. *Calamintha nepeta* L.
670 (Savi) as source of phytotoxic compounds: bio-guided fractionation in identifying biological
671 active molecules. *Acta Physiol. Plant.* **2013**, *35* (6), 1979–1988.
- 672 (36) Tambone, F.; Scaglia, B.; D’Imporzano, G.; Schievano, A.; Orzi, V.; Salati, S.; Adani, F.
673 Assessing amendment and fertilizing properties of digestates from anaerobic digestion
674 through a comparative study with digested sludge and compost. *Chemosphere* **2010**, *81* (5),
675 577–583.
- 676 (37) Massaccesi, L.; Sordi, A.; Micale, C.; Cucina, M.; Zadra, C.; Di Maria, F.; Gigliotti, G.
677 Chemical characterisation of percolate and digestate during the hybrid solid anaerobic
678 digestion batch process. *Process Biochem.* **2013**, *48* (9), 1361–1367.
- 679 (38) Cuetos, M. J.; Morán, A.; Otero, M.; Gómez, X. Anaerobic co-digestion of poultry blood
680 with OFMSW: FTIR and TG-DTG study of process stabilization. *Environ. Technol.* **2009**, *30*
681 (6), 571–582.
- 682 (39) Provenzano, M. R.; Iannuzzi, G.; Fabbri, C.; Senesi, N. Qualitative characterization and
683 differentiation of digestates from different biowastes using FTIR and fluorescence
684 spectroscopies. *J. Environ. Prot. (Irvine, Calif.)*. **2011**, *2* (01), 83–89.
- 685 (40) Provenzano, M. R.; Malerba, A. D.; Pezzolla, D.; Gigliotti, G. Chemical and spectroscopic
686 characterization of organic matter during the anaerobic digestion and successive composting

- 687 of pig slurry. *Waste Manage.* **2014**, *34* (3), 653–660.
- 688 (41) Zhou, W.; Gao, J.; Zhao, H.; Meng, X.; Wu, S. The role of quinone cycle in Fe^{2+} - H_2O_2
689 system in the regeneration of Fe^{2+} . *Environ. Technol.* **2017**, *38* (15), 1887–1896.
- 690 (42) Bokare, A. D.; Choi, W. Review of iron-free Fenton-like systems for activating H_2O_2 in
691 advanced oxidation processes. *J. Hazard. Mater.* **2014**, *275*, 121–135.
- 692 (43) Pilli, S.; Yan, S.; Tyagi, R. D.; Surampalli, R. Y. Overview of Fenton pre-treatment of sludge
693 aiming to enhance anaerobic digestion. *Rev. Environ. Sci. Biotechnol.* **2015**, *14* (3), 453–472.
- 694 (44) Xu, H. Y.; Liu, W. C.; Qi, S. Y.; Li, Y.; Zhao, Y.; Li, J.-W. Kinetics and optimization of the
695 decoloration of dyeing wastewater by a schorl-catalyzed Fenton-like reaction. *J. Serb. Chem.*
696 *Soc.* **2014**, *79* (3), 361–377.
- 697 (45) Nam, K.; Rodriguez, W.; Kukor, J. J. Enhanced degradation of polycyclic aromatic
698 hydrocarbons by biodegradation combined with a modified Fenton reaction. *Chemosphere*
699 **2001**, *45* (1), 11–20.
- 700 (46) Wu, Y.; Zhou, S.; Ye, X.; Zhao, R.; Chen, D. Oxidation and coagulation removal of humic
701 acid using Fenton process. *Colloids Surf., A* **2011**, *379* (1–3), 151–156.
- 702 (47) Catrouillet, C.; Davranche, M.; Dia, A.; Bouhnik-Le Coz, M.; Marsac, R.; Pourret, O.;
703 Gruau, G. Geochemical modeling of $\text{Fe}(\text{II})$ binding to humic and fulvic acids. *Chem. Geol.*
704 **2014**, *372*, 109–118.
- 705 (48) Nuzzo, A.; Sánchez, A.; Fontaine, B.; Piccolo, A. Conformational changes of dissolved
706 humic and fulvic superstructures with progressive iron complexation. *J. Geochemical Explor.*
707 **2013**, *129*, 1–5.
- 708 (49) Piccolo, A. The supramolecular structure of humic substances. *Soil Sci.* **2001**, *166* (11), 810–
709 832.
- 710 (50) Sánchez, M.; Gomez, X.; Barriocanal, G.; Cuetos, M. J.; Morán, A. Assessment of the
711 stability of livestock farm wastes treated by anaerobic digestion. *Int. Biodeterior. Biodegrad.*
712 **2008**, *62* (4), 421–426.

- 713 (51) Lencioni, G.; Imperiale, D.; Cavirani, N.; Marmiroli, N.; Marmiroli, M. Environmental
714 application and phytotoxicity of anaerobic digestate from pig farming by in vitro and in vivo
715 trials. *Int. J. Environ. Sci. Technol.* **2016**, *13* (11), 2549–2560.
- 716 (52) Marchiol, L.; Mondini, C.; Leita, L.; Zerbi, G. Effects of municipal waste leachate on seed
717 germination in soil-compost mixtures. *Restor. Ecol.* **1999**, *7* (2), 155–161.
- 718 (53) Komilis, D. P.; Tziouvaras, I. S. A Statistical analysis to assess the maturity and stability of
719 six composts. *Waste Manage.* **2009**, *29* (5), 1504–1513.
- 720 (54) Nasri, N.; Maatallah, S.; Kaddour, R.; Lachâal, M. Effect of salinity on *Arabidopsis thaliana*
721 seed germination and acid phosphatase activity. *Arch. Biol. Sci.* **2016**, *68* (1), 17–23.
- 722 (55) Jia, C.; Kudsk, P.; Mathiassen, S. K. Joint action of benzoxazinone derivatives and phenolic
723 acids. *J. Agric. Food Chem.* **2006**, *54* (4), 1049–1057.
- 724 (56) Reigosa, M. J.; Souto, X. C.; González, L. Effect of phenolic compounds on the germination
725 of six weeds species. *Plant Growth Regul.* **1999**, *28* (2), 83–88.
- 726 (57) Abenavoli, M. R.; Nicolò, A.; Lupini, A.; Oliva, S.; Sorgonà, A. Effects of different
727 allelochemicals on root morphology of *Arabidopsis thaliana*. *Allelopath. J.* **2008**, *22* (1),
728 245–250.
- 729 (58) Trevisan, S.; Francioso, O.; Quaggiotti, S.; Nardi, S. Humic substances biological activity at
730 the plant-soil interface: from environmental aspects to molecular factors. *Plant Signal.*
731 *Behav.* **2010**, *5* (6), 635–643.
- 732 (59) Nieto, L. M.; Hodaifa, G.; Rodríguez, S.; Giménez, J. A.; Ochando, J. Degradation of
733 organic matter in olive-oil mill wastewater through homogeneous Fenton-like reaction.
734 *Chem. Eng. J.* **2011**, *173* (2), 503–510.

735

736 **Figure captions**

737 **Figure 1.** FT-IR spectra of the solid anaerobic digestate before and after the iron-based Fenton
738 stabilization process carried out using different dosages of Fenton reagents (treatments as reported in
739 Table 2).

740

741 **Figure 2.** FT-IR spectra of humic (HA) (a) and fulvic acid (FA) (b) fractions extracted from the solid
742 anaerobic digestate before and after the iron-based Fenton stabilization process carried out using
743 different dosages of Fenton reagents (treatments as reported in Table 2).

744

745 **Figure 3.** Changes in corrected weight losses obtained from Eq. (1) corresponding to DTG2 and
746 DTG3 of a) solid anaerobic digestate and its b) humic and c) fulvic fractions before and after the iron-
747 based Fenton stabilization process carried out using different dosages of Fenton reagents (treatments
748 as reported in Table 2).

749

750 **Figure 4.** Dose-response curve of the germination index [GI (%)] (mean \pm SE, $n = 5$) of seeds of
751 *Lactuca sativa* L. exposed for 48 h under controlled growth conditions (darkness, 25 ± 1 °C) to
752 increasing aqueous extract concentrations (namely 0, 0.1, 1, 5, 10, 20, 80 and 100%) of untreated
753 solid anaerobic digestate (Dig). Different lowercase letters indicate significant differences among
754 treatments ($P < 0.05$). Fitting of the non-linear regression model to estimate the ED₅₀ value (i.e. the
755 percent extract dose determining a 50% reduction of the maximum GI response) was at a significant
756 value of $P < 0.001$.

757

758 **Figure 5.** Variation of the germination index [GI (%)] (mean \pm SE, $n = 5$) of seeds of *Lactuca sativa*
759 L. exposed for 48 h under controlled growth conditions (darkness, 25 ± 1 °C) to increasing aqueous
760 extracts concentrations of solid anaerobic digestate before and after the iron-based Fenton

761 stabilization process carried out using different dosages of Fenton reagents (treatments as reported in
762 Table 2). The significant effect due to the aqueous extract concentration (C) is shown as *F*-value and
763 level of significance (* $P < 0.05$, ** $P < 0.01$, *** $P < 0.001$; ns, not significant) estimated by a one-
764 way ANOVA.
765

ACCEPTED MANUSCRIPT

766 **Table 1. Chemical, biochemical and biological characterization of a solid anaerobic digestate**
 767 **from a medium-scale biogas producing plant^a**

| Parameter | Value |
|--|---------------|
| pH ^b | 8.45 ± 0.03 |
| EC (dS m ⁻¹ at 25°C) ^c | 1.48 ± 0.01 |
| Dry matter (% fresh weight) | 33.5 ± 1 |
| Ash (%) | 10 ± 1 |
| Volatile solids (%) | 90 ± 1 |
| Total C (g kg ⁻¹) | 467.6 ± 0.8 |
| Total N (g kg ⁻¹) | 12.2 ± 0.1 |
| C/N | 38.3 ± 3.2 |
| C _{HA} (%) | 10.98 ± 0.16 |
| C _{FA} (%) | 6.88 ± 1.28 |
| NH ₄ ⁺ -N (g kg ⁻¹) | 1.44 ± 0.13 |
| NH ₄ ⁺ -N (% Total N) | 11.8 ± 1.7 |
| NO ₃ ⁻ -N (g kg ⁻¹) | 0.017 ± 0.001 |
| BOD ₅ (mg L ⁻¹) | 1850 ± 25 |
| Total K (g kg ⁻¹) | 9.06 ± 0.09 |
| Total S (g kg ⁻¹) | 2.00 ± 0.04 |
| Cd (mg kg ⁻¹) | <0.1 |
| Cr _{VI} (mg kg ⁻¹) | 2.48 ± 0.04 |
| Pb (mg kg ⁻¹) | 1.57 ± 0.06 |
| Ni (mg kg ⁻¹) | 1.44 ± 0.06 |
| Hg (mg kg ⁻¹) | <1.5 |
| Cu (mg kg ⁻¹) | 20.60 ± 0.06 |
| Zn (mg kg ⁻¹) | 90.13 ± 0.06 |
| <i>Salmonella</i> spp. | Absent |
| <i>Escherichia coli</i> (CFU g ⁻¹) | Absent |
| Dehydrogenase activity (µg INTF g ⁻¹ 2 h ⁻¹) | 35.7 ± 1.1 |
| FDA-hydrolase activity (µg fluorescein g ⁻¹ h ⁻¹) | 261.0 ± 2.1 |
| Alkaline phosphatase activity (µg p-NP g ⁻¹ h ⁻¹) | 172.2 ± 6.2 |

768 ^a Values are the mean ± SD (n=3) expressed on a dry matter basis.

769 ^b Biomass/H₂O, 3:50, w/v.

770 ^c Biomass/H₂O, 1:10, w/v.

771

772 **Table 2. Dosages of Fenton reagents used in the chemical stabilization process of a solid**
773 **anaerobic digestate from a medium-scale biogas producing plant. Reactions were carried out**
774 **using a laboratory-scale air-tight glass reactor (as shown in Figure S1) operating at pH 3.0,**
775 **internal pressure -100 mbar, temperature 70 °C, stirring speed 50 rpm, for 8 h**

| Treatment | Fenton reagent dosage | | H ₂ O ₂ /Fe ²⁺ ratio |
|------------------|--|---|---|
| | Fe ²⁺ (mg L ⁻¹) | H ₂ O ₂ (mg L ⁻¹) | |
| Dig ^a | 0 | 0 | 0 |
| Ctrl | 0 | 0 | 0 |
| A1 | 846 | 0 | 0 |
| A2 | 846 | 6.03 | 0.0071 |
| A3 | 846 | 12.06 | 0.0143 |
| A4 | 846 | 18.09 | 0.0214 |
| A5 | 846 | 24.12 | 0.0286 |
| B1 | 1692 | 0 | 0 |
| B2 | 1692 | 6.03 | 0.0036 |
| B3 | 1692 | 12.06 | 0.0071 |
| B4 | 1692 | 18.09 | 0.0107 |
| B5 | 1692 | 24.12 | 0.0143 |

776 ^a Physically and chemically untreated solid anaerobic digestate was taken as a reference treatment.

777 **Table 3. Selected physical and chemical properties of the solid anaerobic digestate before (Dig) and after the iron-based Fenton process**
 778 **carried out using different dosages of Fenton reagents^a**

| Treatment ^b | BSI ^c | EC _{1:10} (dS m ⁻¹) | TPC ^d (mg kg ⁻¹) | OM ^e (%) | C (%) | N (%) | C/N |
|------------------------|------------------|---|--|------------------------|--------------|---------------|--------------|
| Dig | 3 | 1.48 ± 0.02 k | 363.2 ± 17.9 a | 91.7 ± 2.6 | 46.8 ± 0.3 a | 1.22 ± 0.01 a | 38.3 ± 0.3 c |
| Ctrl | 3 | 1.43 ± 0.02 k | 250.5 ± 9.1 b | 91.3 ± 2.2 | 46.1 ± 0.9 a | 0.99 ± 0.10 b | 46.5 ± 1.2 b |
| A1 | 3 | 1.56 ± 0.02 j | 183.0 ± 3.4 c | 91.7 ± 1.7 | 47.2 ± 0.8 a | 0.99 ± 0.06 b | 47.7 ± 0.9 b |
| A2 | 2 | 1.84 ± 0.03 i | 111.2 ± 1.9 d | 91.1 ± 1.2 | 47.3 ± 0.4 a | 0.99 ± 0.09 b | 47.8 ± 0.8 b |
| A3 | 2 | 2.04 ± 0.02 h | 95.6 ± 1.8 e | 91.5 ± 1.7 | 47.1 ± 0.7 a | 0.99 ± 0.04 b | 47.7 ± 1.4 b |
| A4 | 1 | 2.48 ± 0.02 f | 85.0 ± 1.6 f | 90.8 ± 1.5 | 47.3 ± 0.3 a | 1.01 ± 0.05 b | 46.8 ± 0.9 b |
| A5 | 1 | 2.30 ± 0.02 g | 45.3 ± 4.4 g | 89.2 ± 1.2 | 47.4 ± 0.4 a | 1.00 ± 0.05 b | 47.6 ± 0.8 b |
| B1 | 3 | 2.66 ± 0.02 e | 179.7 ± 3.3 c | 88.8 ± 2.3 | 47.2 ± 0.5 a | 0.97 ± 0.01 b | 48.7 ± 0.6 a |
| B2 | 3 | 3.49 ± 0.03 c | 117.8 ± 5.1 d | 91.2 ± 1.0 | 47.3 ± 0.6 a | 1.01 ± 0.05 b | 46.4 ± 0.7 b |
| B3 | 3 | 3.23 ± 0.02 d | 101.6 ± 7.3 e | 90.7 ± 1.1 | 47.3 ± 0.1 a | 1.02 ± 0.06 b | 46.8 ± 0.6 b |
| B4 | 1 | 3.92 ± 0.02 b | 69.3 ± 2.4 fg | 90.0 ± 1.3 | 47.7 ± 0.3 a | 0.96 ± 0.09 b | 49.7 ± 1.0 a |
| B5 | 1 | 4.20 ± 0.02 a | 43.8 ± 2.7 g | 90.1 ± 2.0 | 47.3 ± 0.3 a | 0.97 ± 0.09 b | 48.8 ± 0.9 a |

779 ^a Values are mean ± SD (*n*=3) expressed on a dry matter basis. Lowercase different letters indicate significant differences among treatments (*P* <
 780 0.05).

781 ^b Treatments as reported in Table 2.

782 ^c Bad odor index

783 ^d Total phenolic compound content, expressed as catechol

784 ^e Organic matter by weight loss on ignition.

785 **Table 4. Yield and elemental analysis of humic and fulvic acid fractions extracted from a**
 786 **solid anaerobic digestate before (Dig) and after the iron-based Fenton stabilization**
 787 **carried out using different dosages of Fenton reagents^a**

| Treatment ^b | Extraction yield (%) | C (%) | N (%) |
|------------------------|----------------------|----------------|---------------|
| <i>Humic acids</i> | | | |
| Dig | 3.7 | 43.06 ± 0.19 a | 5.97 ± 0.07 a |
| Ctrl | 3.9 | 43.04 ± 0.18 a | 5.92 ± 0.07 a |
| A1 | 3.0 | 41.44 ± 0.23 c | 5.42 ± 0.10 b |
| A2 | 4.1 | 41.21 ± 0.40 c | 5.29 ± 0.10 b |
| A3 | 5.6 | 42.26 ± 0.20 b | 5.33 ± 0.25 b |
| A4 | 7.6 | 42.57 ± 0.07 b | 5.26 ± 0.07 b |
| A5 | 6.5 | 42.59 ± 0.19 b | 5.22 ± 0.22 b |
| B1 | 3.0 | 41.80 ± 0.28 c | 4.72 ± 0.08 c |
| B2 | 3.8 | 37.98 ± 0.34 d | 4.57 ± 0.12 c |
| B3 | 3.0 | 38.66 ± 0.39 d | 4.75 ± 0.04 c |
| B4 | 4.9 | 41.23 ± 0.44 c | 4.12 ± 0.07 d |
| B5 | 5.4 | 41.32 ± 0.35 c | 4.10 ± 0.07 d |
| <i>Fulvic acids</i> | | | |
| Dig | 0.9 | 40.50 ± 0.42 a | 4.80 ± 0.14 a |
| Ctrl | 2.7 | 33.25 ± 0.57 d | 4.09 ± 0.03 b |
| A1 | 3.4 | 33.19 ± 0.37 d | 3.38 ± 0.06 c |
| A2 | 3.7 | 33.40 ± 0.32 d | 3.08 ± 0.05 d |
| A3 | 4.2 | 34.60 ± 0.21 c | 2.88 ± 0.01 e |
| A4 | 4.6 | 35.42 ± 0.43 b | 2.68 ± 0.01 f |
| A5 | 2.8 | 35.66 ± 0.24 b | 2.63 ± 0.10 f |
| B1 | 2.7 | 33.05 ± 0.17 d | 3.46 ± 0.07 c |
| B2 | 2.2 | 34.64 ± 0.13 c | 3.41 ± 0.07 c |
| B3 | 2.3 | 35.91 ± 0.10 b | 3.39 ± 0.08 c |
| B4 | 5.4 | 35.89 ± 0.23 b | 3.23 ± 0.01 d |
| B5 | 3.4 | 35.80 ± 0.20 b | 3.20 ± 0.01 d |

788 ^a Values are mean ± SD (n=3) expressed on a dry matter basis. Lowercase different letters
 789 indicate significant differences among treatments within the same extracted fraction (*P* < 0.05).

790 ^b Treatments as reported in Table 2.

791 **Table 5. Wavenumber and assignment of main absorbance bands in FT-IR spectra**

| Wavenumber (cm ⁻¹) | Assignment |
|--------------------------------|--|
| 3300-3400 | OH of phenols, alcohols and carboxylic groups |
| 2847-2955 | C-H stretching of alkyl structures |
| 1710-1772 | C=O stretching in carboxyl groups, carboxylic acids and ketones |
| 1590-1686 | Aromatic C=C, C=O in amides I, ketone and quinones |
| 1508-1560 | N-H stretching of amide II |
| 1444-1460 | C-H stretching in aliphatic structures |
| 1394-1430 | OH of phenols, COO ⁻ , -CH ₃ |
| 1370-1381 | COO ⁻ antisymmetric stretching, C-H and bending of CH ₂ and CH ₃ groups |
| 1220-1240 | amide III or aromatic ethers |
| 1198 | C-O stretching and OH deformation of COOH |
| 1090-1270 | C-O stretching of aryl ethers and phenols, C-O stretching of secondary alcohols |
| 1034-1040 | C-H stretching of polysaccharides |
| 874-896 | C-O bonds in the carbonate ion |

792

793

794

For Table of Contents Only

795

